Climatology of Daily Precipitation and Extreme Precipitation Events in the Northeast United States

LAURIE AGEL,[*,+] MATHEW BARLOW,[*,#] JIAN-HUA QIAN,[*] FRANK COLBY,[*,@] ELLEN DOUGLAS,[&] AND TIMOTHY EICHLER[**]

[*] *Department of Environmental, Earth, and Atmospheric Sciences, University of Massachusetts Lowell, Lowell, Massachusetts*
[+] *Intercampus Marine Science Graduate Program, University of Massachusetts Lowell, Lowell, Massachusetts*
[#] *Climate Change Initiative, University of Massachusetts Lowell, Lowell, Massachusetts*
[@] *Wind Energy Research Group, University of Massachusetts Lowell, Lowell, Massachusetts*
[&] *School for the Environment, University of Massachusetts Boston, Boston, Massachusetts*
[**] *Earth and Atmospheric Sciences, University of St. Louis, St. Louis, Missouri*

(Manuscript received 29 July 2014, in final form 15 May 2015)

ABSTRACT

This study examines U.S. Northeast daily precipitation and extreme precipitation characteristics for the 1979–2008 period, focusing on daily station data. Seasonal and spatial distribution, time scale, and relation to large-scale factors are examined. Both parametric and nonparametric extreme definitions are considered, and the top 1% of wet days is chosen as a balance between sample size and emphasis on tail distribution. The seasonal cycle of daily precipitation exhibits two distinct subregions: inland stations characterized by frequent precipitation that peaks in summer and coastal stations characterized by less frequent but more intense precipitation that peaks in late spring as well as early fall. For both subregions, the frequency of extreme precipitation is greatest in the warm season, while the intensity of extreme precipitation shows no distinct seasonal cycle. The majority of Northeast precipitation occurs as isolated 1-day events, while most extreme precipitation occurs on a single day embedded in 2–5-day precipitation events. On these extreme days, examination of hourly data shows that 3 h or less account for approximately 50% of daily accumulation. Northeast station precipitation extremes are not particularly spatially cohesive: over 50% of extreme events occur at single stations only, and 90% occur at only 1–3 stations concurrently. The majority of extreme days (75%–100%) are related to extratropical storms, except during September, when more than 50% of extremes are related to tropical storms. Storm tracks on extreme days are farther southwest and more clustered than for all storm-related precipitation days.

1. Introduction

Extreme precipitation has large societal impacts and appears to be increasing with climate change in many regions of the United States (Melillo et al. 2014). The goal of this paper is to examine the characteristics of U.S. Northeast daily precipitation and extreme precipitation in terms of the seasonal and spatial distribution of intensity and frequency, time scale, and relation to large-scale factors in terms of extratropical and tropical cyclone storm tracks. We focus on the Northeast to allow a detailed look at a specific region, here defined as the states of New York (NY), Connecticut (CT), Rhode Island (RI), Massachusetts (MA), Vermont (VT), New Hampshire (NH), and Maine (ME). Most previous work (detailed below) has examined Northeast precipitation characteristics primarily within continental-to-global-scale analyses using diverse methods and data sources, making results difficult to compare because of differences in precipitation sources, time scales, spatial resolutions (station vs gridded), definitions of extremes, and methods of attribution to physical mechanisms. In this study, we consider multiple characteristics of extreme precipitation using a single extreme definition (top 1%) and dataset (30 yr of selected daily station data in the Northeast). Station data are used to avoid issues associated with interpolation in gridded data. A similar analysis for all daily precipitation (herein referred to as ''overall precipitation'') is also conducted to

Corresponding author address: Laurie Agel, Department of Environmental, Earth, and Atmospheric Sciences, University of Massachusetts Lowell, 1 University Avenue, Lowell, MA 01854.
E-mail: laurie_agel@student.uml.edu

DOI: 10.1175/JHM-D-14-0147.1

provide the framework from which to evaluate extreme precipitation.

Extreme precipitation in the Northeast can have significant impacts on infrastructure, property, local economies, and human health. These impacts occur year-round, because of combined rain, snow, snowmelt, convective storms, tropical storms, and extratropical storms. Significant extreme precipitation events include Hurricane Bob in 1991, which caused $1.5 billion in damages and 18 deaths in coastal North Carolina, Long Island, and New England; the Blizzard of January 1996 over the Appalachians, mid-Atlantic, and Northeast, which included severe flooding caused by rain and snowmelt and caused $3 billion in damages and 187 deaths (Lott and Ross 2006); Hurricane Floyd in 1999, which caused $6 billion in damages and 77 deaths on its path from the mid-Atlantic through New England (NOAA 2015); and, more recently, flooding in May 2006, which caused over $70 million in damages in Massachusetts alone (Federal Emergency Management Agency 2006), and Hurricane Irene in 2011, which caused nearly $7 billion in damages (Melillo et al. 2014), much of it in the state of Vermont.

The costs and impacts of extreme precipitation events may be magnified in the future because of climate change (Melillo et al. 2014). Based on observations, there is a statistically significant upward trend in the frequency and intensity of Northeast extreme precipitation from 1958 to 2010 (Kunkel et al. 2013a, 1999; DeGaetano 2009; Pryor et al. 2009). Other studies show a pronounced increase in maximum precipitation in the last two decades at several coastal Northeast stations (Douglas and Fairbank 2011) and an increase of the wettest 95% of days since 1960 at selected Northeast stations (Griffiths and Bradley 2007). Despite substantial decadal-scale variability, these trends are particularly strong for fall and annual periods (Kunkel et al. 2013b). Climate models also show upward trends in Northeast precipitation extremes: a combination of phase 3 of the Coupled Model Intercomparison Project (CMIP3) and North American Regional Climate Change Assessment Program (NARCCAP) climate model simulations using the A2 high-emission scenario show increases in the number of days of precipitation over 25.4 mm (Kunkel et al. 2013b). These observational and simulated precipitation trends serve as the backdrop to a documented increase in Northeast flooding (Peterson et al. 2013).

Aspects of Northeast extreme precipitation have been examined in previous studies through regional analyses embedded as part of larger United States–wide or global studies. Spatial scale is considered by Konrad (2001), who found by examining 2-day station-based contiguous precipitation areas that Northeast extreme precipitation is composed mostly of small-scale events covering less than 2500 km^2. Relationships of extreme precipitation to extratropical and tropical cyclones are considered by Barlow (2011), Kunkel et al. (2012), Pfahl and Wernli (2012), and Hawcroft et al. (2012). Barlow (2011) found that 40%–60% of the wettest days at National Climatic Data Center (NCDC) Global Daily Climatology Network stations in the Northeast are associated with hurricanes. Using threshold levels associated with 5-yr return values, Kunkel et al. (2012) attributed annual extreme Northeast precipitation to 47% frontal processes, 36% tropical cyclones, and 16% extratropical cyclones. Pfahl and Wernli (2012) estimated that 60%–80% of Northeast gridded 6-hourly 99th percentile precipitation is associated with cyclone centers (based on ERA-Interim sea level pressure analysis), and 20%–30% of the annual cyclones occurring during December–February (DJF) contribute 90%–100% of DJF extreme precipitation. Hawcroft et al. (2012), using ERA-Interim 850-hPa relative vorticity, estimated that storms contribute approximately 85% of total precipitation in DJF, and the most heavily precipitating 10% of cyclones contribute over 20% of total storm-associated precipitation. The role of fronts related to extratropical storms has also been examined. Using an objective front identification algorithm based on 850-hPa wet-bulb temperature gradients, Catto et al. (2012) estimated that over 28% of precipitation is associated with cold fronts and 29% with warm fronts in the midlatitudes, and Catto and Pfahl (2013) found that over 90% of extreme precipitation is associated with fronts.

Here, we investigate overall and extreme precipitation in the Northeast in terms of seasonal and spatial distribution, time scale, and relation to large-scale factors using a single extreme definition (top 1%) and dataset (30 yr of selected daily station data). For seasonal and spatial distribution, we identify two distinct Northeast subregions based on the seasonal cycle of intensity, and for each subregion we develop a monthly climatology of frequency, intensity, and total precipitation for both overall and extreme daily precipitation. For time scale, we consider multiday precipitation and develop regional monthly climatologies of overall and extreme multiday precipitation as for daily precipitation; additionally, we examine subdaily precipitation using hourly data. For large-scale factors, we focus on proximity to extratropical and tropical cyclones. We divide daily precipitation into dynamical groupings based on the nearness of extratropical and tropical storm tracks, and we develop regional overall and extreme precipitation climatologies based on these groupings. We then link the extratropical storm–related precipitation to storm-track locations. We

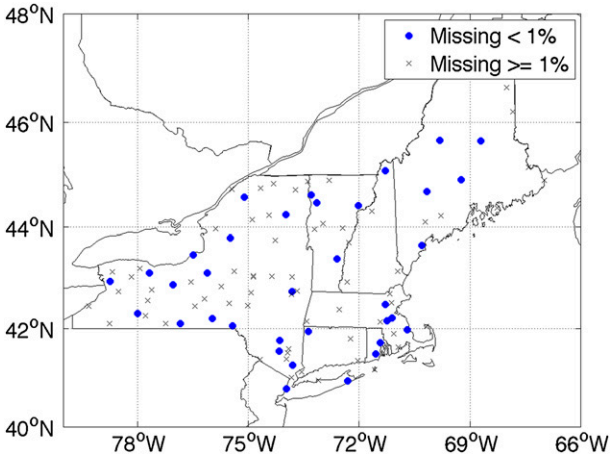

FIG. 1. Northeast USHCN stations missing less than 1% of daily data from 1979 to 2008 (filled blue circles). Additional USHCN stations (missing at least 1% and up to 70% of daily data) are shown with black crosses.

also consider how widespread (affecting the most nearby stations) an extreme precipitation event is for dynamical categories and subregions. Together, these analyses provide a detailed picture of the climatological behavior of overall and extreme daily precipitation in the Northeast.

The remainder of this paper is organized as follows. Data are described in section 2. The results are given in section 3, which is divided into spatial distribution of daily precipitation (section 3a), definition of extreme precipitation (section 3b), seasonal cycles of daily precipitation and extreme daily precipitation (section 3c), multiday and hourly precipitation (section 3d), large-sale factors of daily precipitation (section 3e), storm tracks (section 3f), and spatial cohesiveness (section 3g). The paper concludes with a summary and discussion in section 4.

TABLE 1. Northeast USHCN stations missing less than 1% of daily data from 1979–2008.

Station	Lat (N)	Lon (W)	State	Description
062658	41.9500°	73.3667°	CT	Falls Village
190535	42.4833°	71.2833°	MA	Bedford
190736	42.2122°	71.1136°	MA	Blue Hill
196486	41.9819°	70.6961°	MA	Plymouth–Kingston
198757	42.1608°	71.2458°	MA	Walpole 2
170814	45.6603°	69.8120°	ME	Brassua Dam
171628	44.9197°	69.2417°	ME	Corinna
172765	44.6889°	70.1567°	ME	Farmington
175304	45.6503°	68.7050°	ME	Millinocket
176905	43.6497°	70.3003°	ME	Portland Jetport
272999	45.0875°	71.2872°	NH	First Connecticut Lake
300042	42.7431°	73.8092°	NY	Albany International Airport
300183	42.3017°	77.9889°	NY	Angelica
300687	42.2067°	75.9800°	NY	Binghamton Greater Airport
300889	40.9464°	72.3067°	NY	Bridgehampton
301012	42.9408°	78.7358°	NY	Buffalo Niagara International
301185	44.5772°	75.1097°	NY	Canton 4 southeast
302060	42.0628°	75.4264°	NY	Deposit
302610	42.0997°	76.8358°	NY	Elmira
303184	42.8767°	77.0308°	NY	Geneva Research Farm
304555	44.2444°	73.9847°	NY	Lake Placid 2 south
304912	43.7975°	75.4817°	NY	Lowville
305426	41.7681°	74.1550°	NY	Mohonk Lake
305801	40.7789°	73.9692°	NY	New York City Central Park
306314	43.4622°	76.4933°	NY	Oswego east
307167	43.1167°	77.6767°	NY	Rochester International Airport
308383	43.1092°	76.1033°	NY	Syracuse Hancock International Airport
308906	41.5514°	74.1628°	NY	Walden 1 east-southeast
309670	41.2664°	73.7975°	NY	Yorktown Heights 1 west
374266	41.4906°	71.5414°	RI	Kingston
376698	41.7219°	71.4325°	RI	Providence T.F. Green State Airport
431081	44.4681°	73.1503°	VT	Burlington International Airport
431243	43.3847°	72.5989°	VT	Cavendish
437054	44.4200°	72.0194°	VT	Saint Johnsbury
437607	44.6264°	73.3031°	VT	South Hero

2. Data

a. Precipitation

This study uses station-based daily precipitation observations from the NCDC U.S. Historical Climatology Network (USHCN; Easterling et al. 1999) for the years 1979–2008. The USHCN is a subset of the NCDC Global Historical Climatology Network (GHCN-Daily) product and is composed of high-quality observations from approximately 1200 of the 19 000+ Cooperative Observer (COOP) stations. COOP station observations are excellent choices for studying heavy precipitation events because of their long-term records, standard instrumenation, minimal time-dependent and wind-driven biases, and sufficient spatial coverage (Kunkel et al. 2013a). One disadvantage of the COOP network is an observation schedule (24-h period that composes a day) that varies from station to station and makes intercomparisons of daily precipitation difficult.

For this study, 35 USHCN stations missing no more than 1% of daily data from 1979 to 2008 are used (Fig. 1, blue circles; additional information is in Table 1). Of these, 14 stations are missing no more than 3 consecutive days and no more than 0.2% of daily data. The remaining 21 stations have occasional data gaps between 8 and 31 consecutive days (one station has a single 2-month gap). The impact of the data gaps is minimal, since the 30-yr seasonal precipitation between the top 14 stations and the 35-station set is similar. Hence, the 35-station set is chosen to gain the greatest regional coverage and to maximize the set of

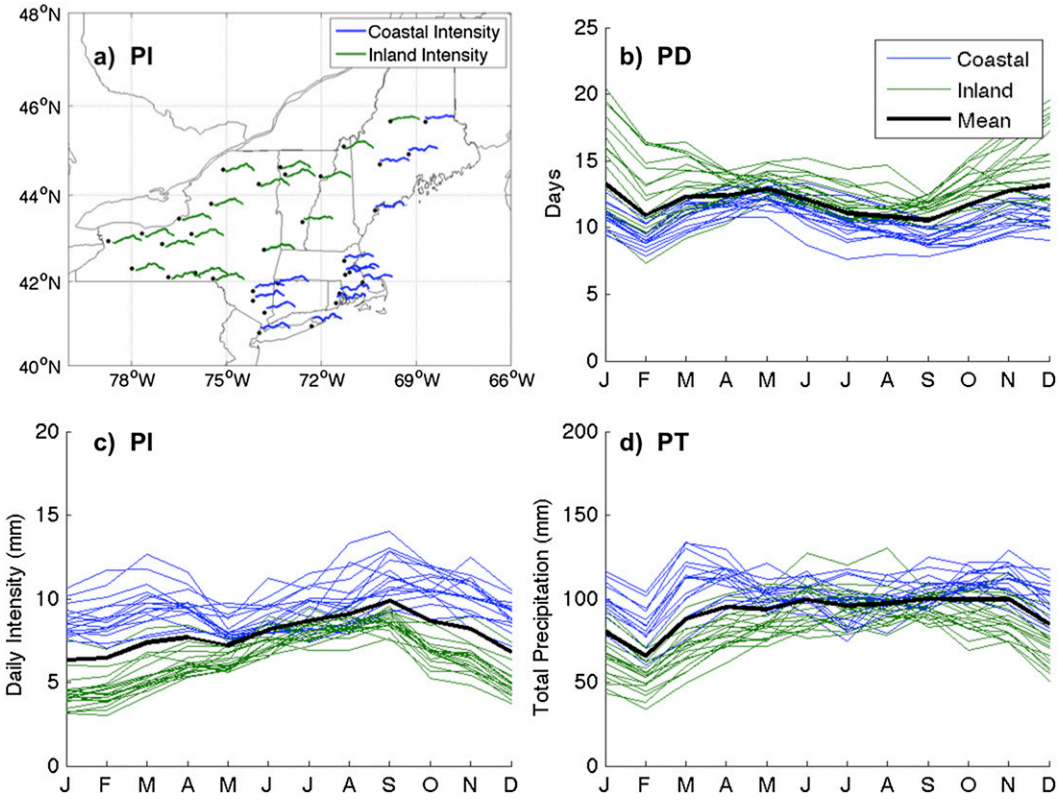

FIG. 2. (a) The geographical separation of Northeast USHCN coastal and inland stations, and the characteristic seasonal cycle of PI for each station. The station seasonal cycles for (b) PD, (c) PI, and (d) PT are also shown. The thick black line shows the mean of all stations, and the colored lines show the individual contribution of each station. Based on the shapes of the seasonal cycles and geographic location, the stations are separated into 16 coastal (blue lines) and 19 inland (green lines) stations.

extreme precipitation days without biasing the results with excessive missing data (between 1% and 70% of days) from the remaining USHCN stations (Fig. 1, black crosses).

Overall precipitation is characterized throughout this study by three parameters: number of days of precipitation (PD), daily precipitation intensity (PI; mm day^{-1}), and precipitation total (PT). PI is based on wet days (precipitation greater than 0.01 in. or 0.254 mm) to best represent the precipitation rate, since including dry days can hide or dilute high rainfall rates at normally dry stations and light rainfall rates at normally wet stations. Similarly, the extreme precipitation parameters examined are days of extreme precipitation (XD), extreme daily intensity (XI; mm day^{-1}), and extreme precipitation total (XT). Extreme precipitation is defined in section 3b.

NCDC Hourly Precipitation Data (HPD; NCDC DSI-3240) for selected USHCN stations are also examined. The HPD are composed of hourly rain gauge accumulation from approximately 5500 National Weather Service, Federal Aviation Administration, and COOP stations.

b. *Hurricane and storm tracks*

Hurricane-track data are from the National Hurricane Center (NHC) revised Atlantic hurricane database (HURDAT2; NOAA 2014; Landsea and Franklin 2013). The revised dataset includes nonsynoptic best-track times, nondeveloping tropical depressions, and best-track wind radii.

Storm tracks (also referred to as "R2 tracks"; T. Eichler 2012, unpublished data) were developed using a modification of the Serreze (1995) and Serreze et al. (1997) scheme to handle 6-hourly data. The storm-track algorithm utilizes NCEP–DOE AMIP-II reanalysis (R2; Kanamitsu et al. 2002) sea level pressure interpolated onto a 250 km × 250 km version of the National Snow and Ice Data Center (NSIDC) Equal-Area Scalable Earth Grid (EASE-Grid; Armstrong and Brodzik 1995).

The HURDAT2 tracks include tropical cyclones, initial track positions of extratropical-transitioned cyclones,

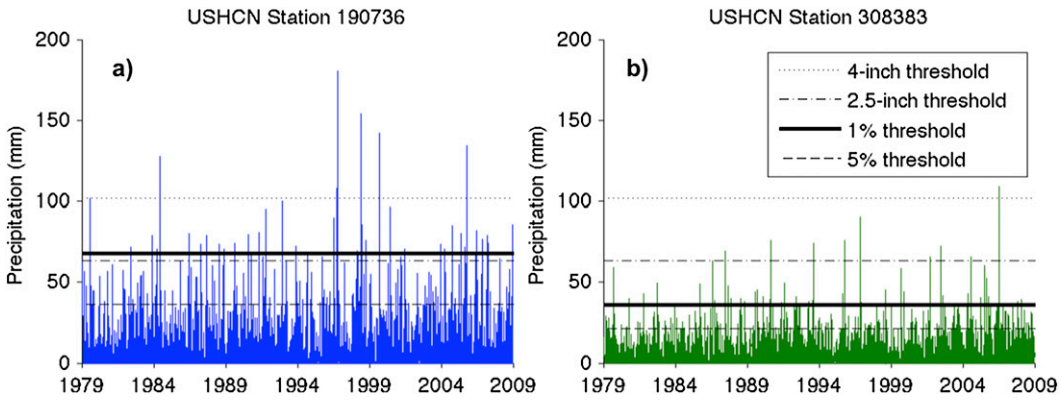

FIG. 3. USHCN daily precipitation time series, 1979–2008, for (a) coastal station 190736 at Blue Hill, MA, and (b) inland station 308383 at Syracuse Hancock International Airport, NY. The 1% wet-day threshold for extreme precipitation at each station is shown with a thick black line. Also shown are the 4-in. (dotted line), 2.5-in. (dotted–dashed line), and top 5% wet-day (dashed line) thresholds.

subtropical cyclones, and tropical disturbances. The R2 tracks contain both tropical and extratropical storms. There is not an exact one-to-one correspondence between tropical R2 tracks and HURDAT2 tracks because of differing algorithms and resolution (e.g., a long-lasting tropical system may be identified in the R2 tracks by a series of several shorter tracks), but visual comparison of HURDAT2 tracks to R2 tracks allows the removal of the tropical tracks from the storm-track database.

3. Results

a. Spatial distribution of daily precipitation

The seasonal cycles of PD, PI, and PT vary considerably across the region. Figure 2a shows the seasonal cycle of PI, the parameter with the largest annual variation, at each station. Two characteristic seasonal cycles in PI are evident: a single peak in late summer and dual peaks in spring and fall. These two shapes also appear to be regionally separated: stations farther inland tend to have single-peaked PI, while stations nearer to the coast tend to have dual-peaked PI. PD also exhibits a regional behavior, with fewer precipitation days inland. Based on the shape of the PI cycle (along with the number of days of precipitation and intensity level where PI is not clearly single peaked or dual peaked), we separate the stations into two subregions with distinct climatologies. Because of the geography of the resulting split, we refer to these subregions as ''inland'' and ''coastal.'' Figures 2b–d show the seasonal cycles of PD, PI, and PT for the 19 inland stations (green lines) and 16 coastal stations (blue lines). Coastal stations tend to have fewer precipitation days and higher daily intensity than inland stations, with dual peaks in PI and PT in spring and fall, as opposed to the single peaks in PI and PT in late summer for inland stations.

We have validated these results in three different ways: by verifying that an independent set of Northeast USHCN stations follow the same separation, by *k*-means clustering, and by a Monte Carlo test of the difference in the seasonal cycles. Using 66 Northeast USHCN stations not chosen for this study (representing independent data), we find that the unused stations also separate into identical subregions based on the shapes of the seasonal cycles of PD, PI, and PT. In addition, a *k*-means cluster analysis using the standardized monthly values of PD and PI and the top 1% threshold (a 35-station by 25-variable matrix) is applied, and this too results in an identical separation into the two subregions. The suitability of a two-cluster solution is objectively confirmed by calculating the classifiability indices of two to five clusters and comparing the indices to those generated by random red noise (Michelangeli et al. 1995). Finally, a Monte Carlo test of the difference in means of 1000 random 16- and 19-station sets indicates that the seasonal cycles of both PD and PI for the selected subregions are significantly different at the 0.05 level, confirming the presence of two distinct precipitation regimes.

Other researchers have also noted regional differences in Northeast precipitation. Tryhorn and DeGaetano (2011) separated this same area into three regions: coastal, northern New England, and western New York. Douglas and Fairbank (2011) used factor groups to distinguish five different precipitation regions in Massachusetts, New Hampshire, and Maine; and several of these factor groups also organized along spatial boundaries. In this study, the monthly climatologies of PD, PI, and PT

separate most distinctly into the two subregions identified; hence, for simplicity we considered a division into only those two regions.

Because of these demonstrated regional differences, all results presented here will distinguish between coastal and inland stations. As a visual aid, figures show coastal results in blue and inland results in green.

b. *Extreme daily precipitation definition*

There are many possible definitions for extreme precipitation events, from block-maxima and peaks-over-threshold approaches (Anagnostopoulou and Tolika 2012; Lenderink et al. 2011; Hitchens et al. 2010; Ralph et al. 2010) to indices that capture duration or intensity (Griffiths and Bradley 2007; Kenyon and Hegerl 2010). In addition, extremes can also be defined over multiple spatial scales and temporal scales (Konrad 2001).

For this study, we choose a peaks-over-threshold approach for daily data and experiment with several thresholds, ultimately choosing the top 1% of wet days. The advantage to peaks-over-threshold is that missing data are not as critical an issue as with block-maxima approaches, and since thresholds can be chosen on a station-by-station basis, the set of extremes can reflect regional variations. This is important for the Northeast, since there is a demonstrated difference in regional precipitation behavior. The disadvantage of this approach is that choosing the threshold to use can be somewhat ambiguous (Kunkel et al. 2013a). There are statistical techniques available to aid in the selection of a threshold, such as mean excess plots, dispersion testing, and threshold testing (Anagnostopoulou and Tolika 2012; Beguería et al. 2011); however, their use is hindered by the assumption that each extreme must be independent and identically distributed, requiring declustering techniques for serially correlated data (Yiou et al. 2008). In practice, many researchers simply choose a nonparametric threshold, such as 95% or 99%, which has the advantage of being easier to explain to the nonscientist (Kunkel et al. 2013a) and provides a balance between capturing the behavior in the tail of the distribution and generating a suitable sample size (Beguería et al. 2011). Here, we take the latter approach and look at two nonparametric thresholds, the top 1% and top 5% of wet days, and two simple parametric thresholds, 2.5 in. (63.5 mm) and 4.0 in. (101.6 mm). Figure 3 shows the 30-yr time series and the four thresholds for two regionally separated stations. For both stations, the 4.0-in. threshold only captures the far-right tail of extreme precipitation, and the top 5% threshold captures many events that are difficult to characterize as extreme. For station 190736 (Blue Hill, MA, a coastal station), the 2.5-in. and top 1% thresholds capture many of the same extremes, while for station 308383 (Syracuse Hancock International Airport, NY, an inland station), the top 1% threshold captures a similar number of extremes as that for the coastal station, but the 2.5-in. threshold captures considerably fewer extremes. To account for these regional variations, the threshold is chosen to be the top 1% of all wet-day precipitation at each station, resulting in a mean threshold of 40.4 mm (corresponding to a return period of 0.65 yr) for inland stations and 62.7 mm (0.79 yr) for coastal stations (Table 2).

TABLE 2. Extreme threshold (top 1% of wet-day precipitation) and corresponding return period for USHCN station data, 1979–2008, separated into inland and coastal groups.

Station	Extreme threshold (mm)	Return period (yr)
Inland		
272999	37.8	0.54
431081	40.4	0.64
431243	49.8	0.68
437054	40.1	0.61
437607	41.1	0.86
170814	43.4	0.70
300042	44.7	0.77
300183	41.7	0.67
300687	41.7	0.62
301012	37.3	0.60
301185	37.6	0.67
302060	42.2	0.62
302610	44.2	0.73
303184	36.8	0.67
304555	37.6	0.59
304912	41.7	0.60
306314	37.8	0.57
307167	36.3	0.60
308383	35.8	0.60
Mean	40.4	0.65
Coastal		
62658	57.1	0.75
374266	72.6	0.83
376698	65.3	0.81
190535	59.2	0.73
190736	67.8	0.75
196486	64.5	0.73
198757	62.7	0.79
171628	50.0	0.86
172765	57.4	0.70
175304	53.3	0.75
176905	67.3	0.77
300889	72.9	0.91
305426	66.0	0.79
305801	69.6	0.81
308906	53.6	0.86
309670	63.0	0.81
Mean	62.7	0.79

The top 1% threshold garners a sample size of 1563 extreme station dates, composed of 34–59 extreme dates for each station, depending on the number of days of

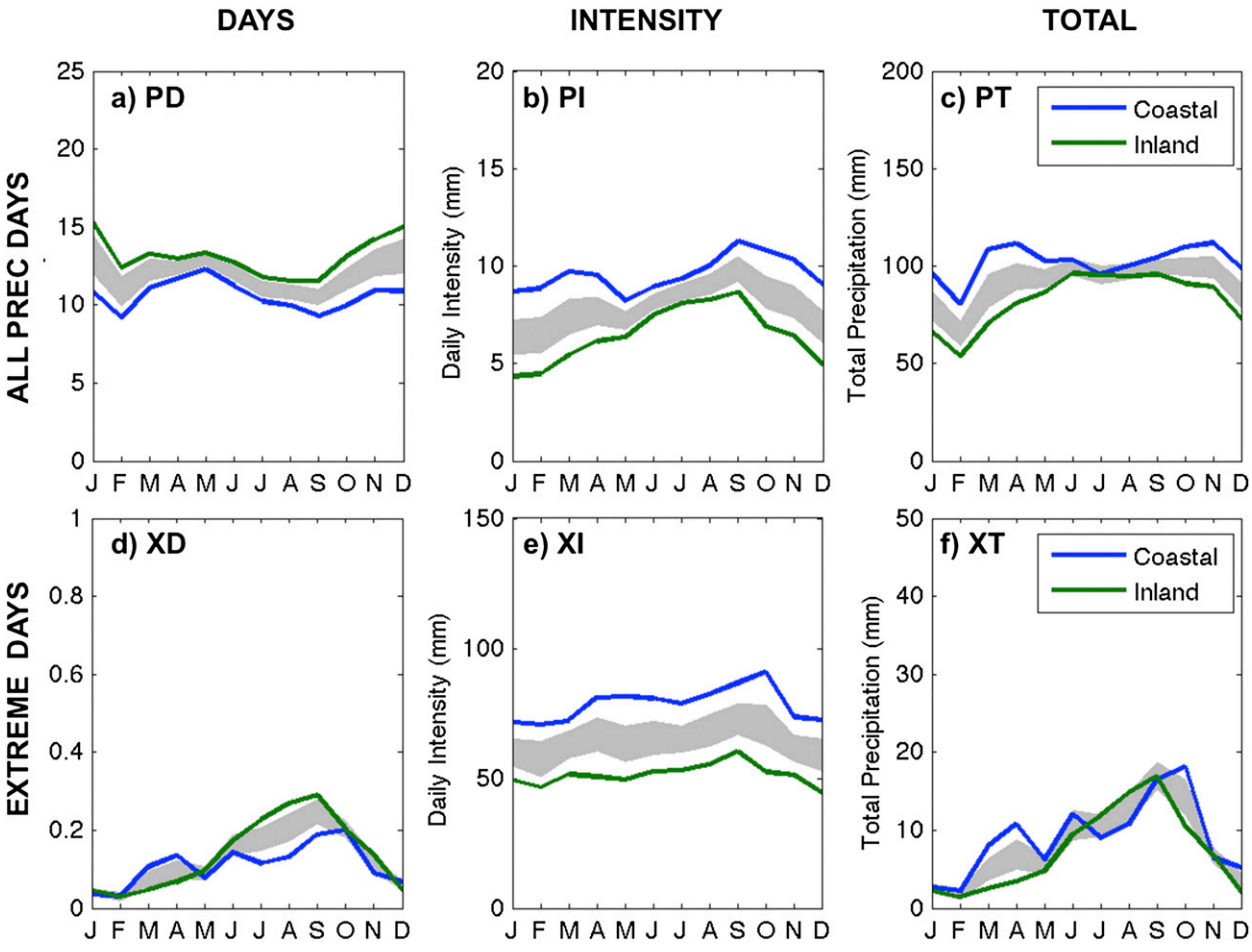

FIG. 4. Mean annual cycles of USHCN overall precipitation and extreme precipitation for the coastal (blue solid line) and inland (green solid line) station sets, 1979–2008. Extreme precipitation is the top 1% of wet days. Shown are (a) PD, (b) PI, (c) PT, (d) XD, (e) XI, and (f) XT. The shaded area indicates the 95% confidence interval of the seasonal cycle using 1000 random samples of 16-station sets.

precipitation at each station during the 30-yr study period. This translates to one or two events of significance per year for each station, which is suitable for daily data (Anagnostopoulou and Tolika 2012). The use of separate seasonal thresholds would increase the number of events per year and have the advantage of allowing cold- and warm-season events to be treated independently. However, for the Northeast, the use of seasonal thresholds does not fundamentally change the results of this study, and the annual threshold is used for simplicity.

c. *Seasonal cycles of daily precipitation and extreme daily precipitation*

The monthly climatologies of PD, PI, and PT are shown in Figs. 4a–c. Seasonal means are shown in Table 3. Annually, inland stations experience more precipitation days than do coastal stations (157 and 128 days, respectively) but less precipitation intensity (6.5 and 9.6 mm day^{-1}, respectively). Seasonally, inland stations experience the highest PD in winter, and the highest PI in September. Coastal stations experience two peaks in PD (one in late spring and a smaller one in late fall) and two peaks in PI (one in early spring and a larger one in September). This manifests in overall less inland PT, except in July, when coastal PT dips to inland levels. It is important to note that the dual peaks in coastal PI and PT appear to be caused by a decrease in midsummer intensity rather than an increase in spring intensity. At least part of the drop in PD and PT in February is caused by the short month, although if normalized to account for number of days in the month, the results are qualitatively similar (i.e., a drop in February). To test the sensitivity of the results to the period tested, we have also calculated the seasonal cycle from 1979–2013 data, and the results are nearly identical. However, because of recent upward trends in extreme precipitation frequency and intensity, particularly during fall (Kunkel et al. 2013b),

TABLE 3. Seasonal and annual (ANN) climatology of overall and extreme precipitation for Northeast USHCN station data, 1979–2008, separated by region. Shown are precipitation days, mean daily precipitation intensity, and total precipitation.

	DJF	MAM	JJA	SON	ANN
Inland overall days					
PD	43	40	36	39	157
PI (mm day^{-1})	4.6	6.0	8.0	7.3	6.5
PT (mm)	193	238	286	276	993
Inland extreme days					
PD	0.12	0.21	0.67	0.63	1.63
PI (mm day^{-1})	47.2	50.2	53.7	54.6	51.8
PT (mm)	6	11	36	34	87
Coastal overall days					
PD	31	35	31	30	128
PI (mm day^{-1})	8.9	9.1	9.4	10.8	9.6
PT (mm)	275	323	299	326	1223
Coastal extreme days					
PD	0.14	0.32	0.39	0.48	1.33
PI (mm day^{-1})	71.8	78.3	80.8	84.0	79.1
PT (mm)	10	25	32	41	108

not all aspects of the seasonal cycles may be stable for future periods.

The difference between inland and coastal cycles of PD and PI is significant at the 0.05 level, based on 1000 random 16-station groupings (gray shading). Inspection of the seasonal cycles for individual years shows strong year-to-year variations, but most years include the characteristic dip in coastal intensity during a portion of the warm season.

The monthly climatologies of XD, XI, and XT are shown in Figs. 4d–f. Seasonal means are shown in Table 3. Annually, inland stations experience 1.63 extreme days per year with intensity of 51.8 mm day^{-1}, while coastal stations experience 1.33 extreme days per year with intensity of 79.1 mm day^{-1}. Seasonally, both inland and coastal stations experience very few extremes in winter and the most extremes in summer and early fall, with more spring extremes at coastal stations. During summer, inland stations experience more extremes than coastal stations. Coastal XI is higher than inland XI for each month, but both have relatively flat seasonal cycles. The XT increases from a seasonal low in winter to a seasonal high in September for inland stations and a seasonal high in October for coastal stations. There are significant differences in inland and coastal XD in March–April and July–September and XT in March–April, based on Monte Carlo random sampling.

d. Other time scales: Multiday precipitation and hourly precipitation

Although this study highlights the climatology of daily precipitation extremes, it is useful to establish the role of daily precipitation in longer-duration extreme precipitation events. A multiday climatology is developed for each Northeast station by assigning each day with precipitation to a precipitation "event" of various durations from 1 to 12 days. An event must be preceded and followed by at least one dry day. A dry day is defined as any day with precipitation less than 0.01 in. (0.254 mm). Each precipitation day belongs to one event only. Extreme multiday events are defined as the top 1% of total event precipitation for the combined set of multiday events. Note that the top 1% multiday events do not necessarily include any top 1% daily precipitation events.

Figure 5a shows the frequency of multiday precipitation event durations. Approximately 50% of precipitation events are isolated single-day events, and over 90% involve precipitation over 1–3 days. The remaining 10% are predominately 4- and 5-day events. The gray shading in Fig. 5a shows the 95% confidence interval of frequency of multiday event durations if the 30-yr time series is randomly shuffled by month (e.g., 30 yr of January days shuffled for each station). The observed results show significantly fewer 1-day events and slightly more multiday events than would be expected by chance.

Figures 5b–d show the mean event intensity, total event precipitation, and maximum daily intensity for event durations of 1–5 days. Coastal event intensity is higher than inland intensity. This is not surprising and is consistent with the results for daily precipitation. Event intensity is remarkably invariant ($\sim$10 mm day^{-1} for coastal stations, $\sim$6 mm day^{-1} for inland stations) despite the lengthening event duration. Total event precipitation is also consistently higher at coastal stations than at inland stations and increases linearly from 1 to 5 days. Maximum intensity increases with event duration (longer-duration events may feature stronger downpours). Based on this, multiday precipitation appears to be composed of one or more days of heavy precipitation embedded in days of lighter precipitation. The gray shading shows the 95% confidence interval of randomly shuffling the daily precipitation among the events 1000 times. The randomized precipitation results are similar to the actual results and confirm that heavy days of precipitation must be interspersed with lighter days of precipitation and account for the higher random values for single-day intensity.

Figure 5e shows the frequency of extreme multiday event durations. In contrast to overall precipitation, where most events are single day, followed by an exponential decrease in larger event duration, most extreme events are 2–5-day events, and the subsequent decrease in frequency with event duration falls at a slower rate. Both coastal and inland stations exhibit

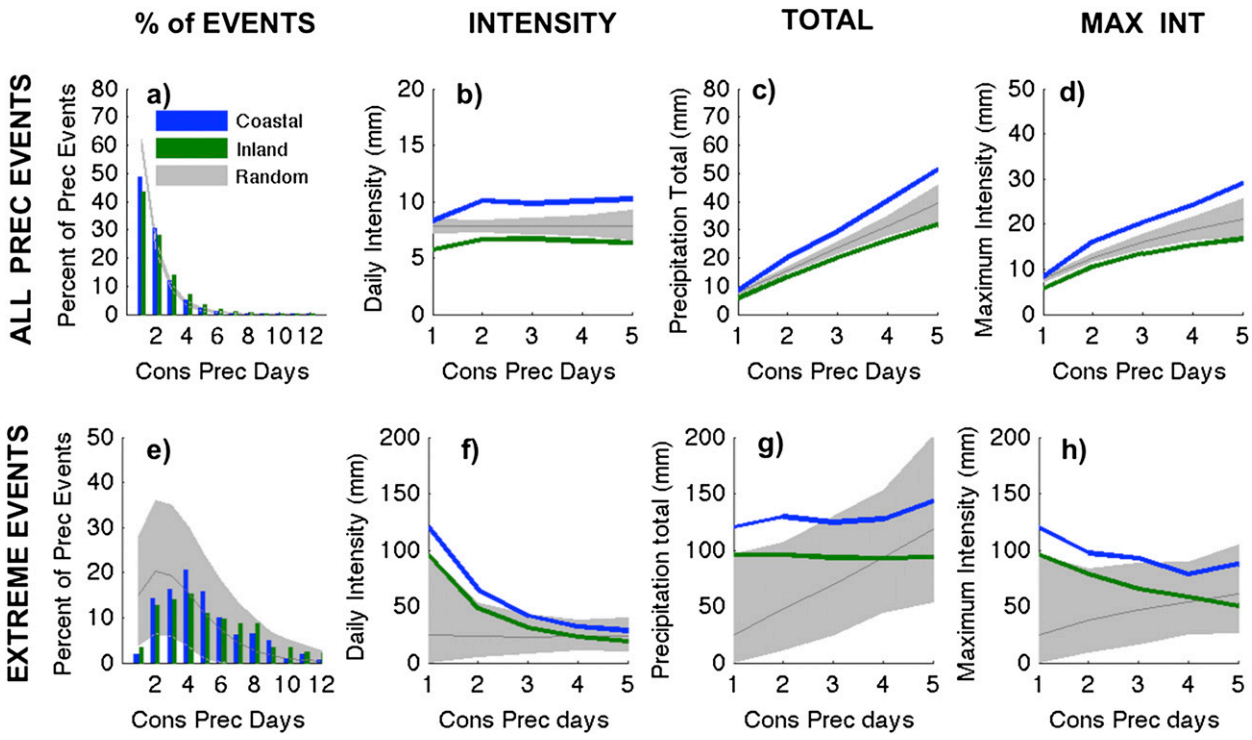

FIG. 5. Characteristics of USHCN multiday precipitation events and extreme multiday precipitation events (top 1% of all multiday precipitation). Shown are (a),(e) frequency of multiday events (%); (b),(f) event mean daily intensity; (c),(g) event total precipitation; and (d),(h) event max daily intensity for (top) all precipitation events and (bottom) extreme precipitation events of various durations. A multiday event consists of consecutive days of at least 0.01 in. (0.254 mm) of precipitation preceded and followed by at least one dry day. Coastal (inland) station data are shown in blue (green). Gray shading in (a) and (e) indicates the mean 95% confidence interval of random shuffling of precipitation days in all years by month for each station. Gray shading in other panels indicates the mean 95% confidence interval of the characteristic from random shuffling of daily precipitation across the multiday events for each station, and the dark gray line indicates the mean value of the random simulations.

peaks in 4-day extreme events. The gray shading shows the 95% confidence interval of frequency of extreme multiday event durations if all precipitation days in the 30-yr time series are randomly shuffled by month, and a new set of extreme events are identified. There are fewer 1-day extreme events (significant) and more longer-duration extreme events (not significant) than would be expected by chance, suggesting that extreme precipitation tends to occur within multiday events.

Extreme event intensity decreases from 100+ mm for single-day events to 20 mm for 5-day events (Fig. 5f), in contrast to overall multiday precipitation, where intensity is 6–10 mm, regardless of event duration. Extreme event total precipitation (Fig. 5g) changes very little with event duration, and maximum event intensity (Fig. 5h) decreases with event duration. The gray shading shows the 95% confidence interval of randomly shuffling the daily precipitation among the extreme events 1000 times. These results differ sharply from those for all precipitation and those from random reassignment of daily precipitation within the extreme events. This may be because of the way in which extreme multiday events are identified: shorter-duration events must have unusually high daily precipitation to be included in the set, and longer-duration events may be included with no individually high precipitation days. In addition, based on this, we can conclude that extreme multiday precipitation follows the pattern of all multiday precipitation, where one or so days contribute the bulk of the total event precipitation, but, in this case, the intensity on that one day is extremely high (which would account for the decreasing intensity but constant total precipitation).

To further investigate this, extreme multiday event duration is compared to the percent of days that are individually considered extreme (99th percentile) within the event (Fig. 6). The dashed line indicates the theoretical curve if only a single day in each event produced extreme precipitation. Nearly 50% of the days in a 2-day event are extreme; nearly 30% of days in 3-day events are extreme; and between 20% and 22% of 4-day events are extreme. This suggests that, at least for 1–5-day

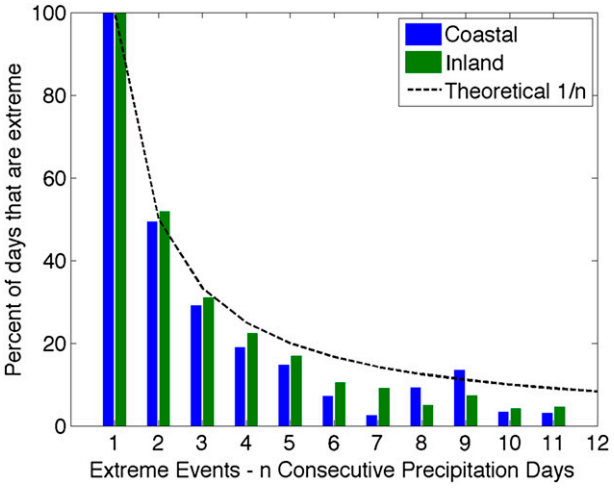

FIG. 6. Percent of extreme days within extreme multiday USHCN precipitation events of up to n = 12-day duration for coastal (blue) and inland (green) stations. Extreme multiday events compose the top 1% of total multiday event precipitation. An extreme day is defined as the top 1% of daily precipitation. The thick dashed line shows the theoretical curve for a single extreme day within each n-day event.

extreme precipitation events, only one extreme precipitation day appears to be embedded in lighter precipitation days. As event duration increases beyond 5 days, the number of embedded extreme days decreases to less than one. This may be an indication that some larger extreme events have no individual extreme days (e.g., the event extremeness is because of total event accumulation); however, this is statistically uncertain, given the small sample sizes for longer-duration events.

To investigate how overall and extreme precipitation occurs on the subdaily scale, the hourly NCDC precipitation for several stations included in both the USHCN daily and NCDC hourly databases is ranked by contribution to total precipitation (Fig. 7). To account for differences in observation schedules between the USHCN daily data and NCDC hourly data, extreme days for this purpose are defined as NCDC midnight-to-midnight precipitation that exceeds the USHCN extreme threshold from Table 2. For overall precipitation, over 80% of the daily precipitation is delivered by the highest-precipitating 3 h; while for extreme precipitation, approximately 50% of the daily precipitation is delivered by the highest-precipitating 3 h. This result is consistent with Hitchens et al. (2010), who found by examining 6-h precipitation in the U.S. Midwest that most subdiurnal extreme precipitation falls within 1–2 h.

To complete this multiday precipitation climatology, the seasonal cycles of the precipitation parameters are developed for inland and coastal station multiday precipitation (Figs. 8 and 9, respectively). For overall precipitation, 1-day events are most frequent in summer and early winter, 2-day events are most frequent in early spring, and 3–5-day events show little seasonal cycle, except for slight increases in late spring and fall. Intensity is similar for each event duration (consistent with increasing single-day maximum intensity per event duration), and there is no pronounced seasonal cycle, although inland stations show a slight increase in summer months. For extreme precipitation, the frequency of event durations appears to be dual peaked, even for inland stations, but peak months differ based on event duration, and no statistical tests are attempted for extreme events as a result of small sample sizes. Extreme intensity decreases with event duration (consistent with a single embedded extreme day), and there is little seasonal cycle. Unsurprisingly, combined 1–5-day event cycles describe the majority of the overall and extreme daily seasonal cycles from Fig. 4.

In summary, although extreme daily precipitation in the Northeast is usually embedded in multiday precipitation events, the intense precipitation is often confined to several hours within a single day, making the use of the partial duration series (daily precipitation) an effective means of measuring extreme precipitation in the Northeast. The remainder of this study will focus on 24-h precipitation extremes.

e. Dynamical categories of daily precipitation

Precipitation days at each station are separated into dynamical groupings of ''hurricane,'' ''storm,'' and ''other,'' based on nearness of the station to HURDAT2 and R2 tracks. A 1000-km radius is used as the criteria for nearness. This radius is based on visual assessment of contiguous precipitation areas and is roughly consistent with previous studies (Kunkel et al. 2012; Barlow 2011; Pfahl and Wernli 2012). If any station experiencing precipitation is within 1000 km of a HURDAT2 track, then precipitation at every station on that day is placed in the hurricane category. For the remainder of precipitation days at each station, the precipitation is assigned to the storm category if the station is within 1000 km of any R2 track on that day; otherwise, the precipitation is assigned to the other category. In this manner, some hurricane precipitation may be related to both tropical cyclone and extratropical storm tracks, but no storm precipitation will be related to tropical cyclone tracks. Because of the 1000-km radius for identification, the extratropical storm category likely contains some events that are distantly related to extratropical storm centers, such as elongated fronts.

Using this technique, out of the 1563 extreme station dates, 292 are attributed to tropical systems (19%), 1036

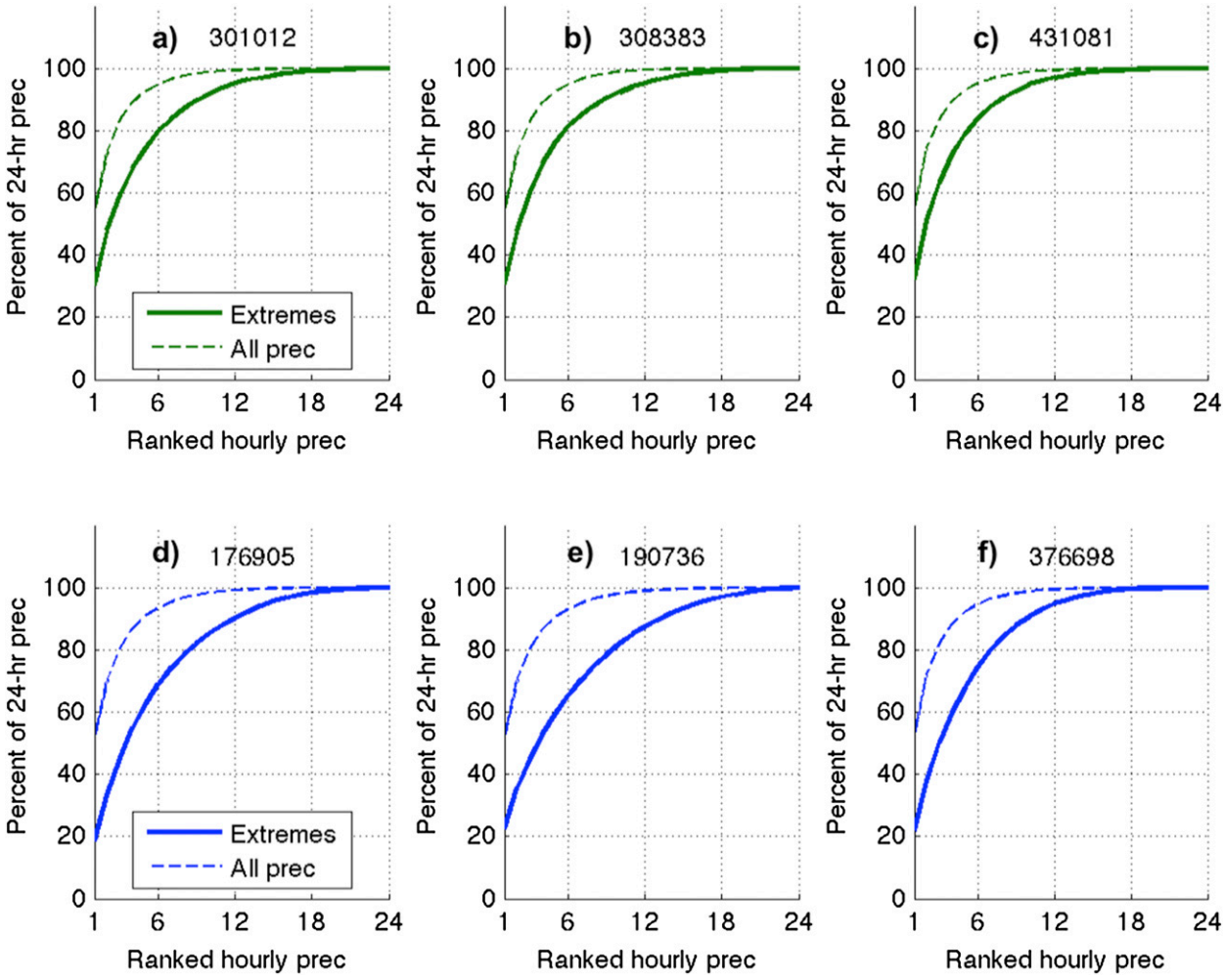

FIG. 7. Cumulative contribution of hourly precipitation to total daily precipitation for selected USHCN stations, using NCDC HPD 24-h totals, 1979–2008. The solid line indicates the cumulative contribution of hourly precipitation on extreme days, and the dashed line indicates the cumulative contribution of hourly precipitation on all precipitation days. Extreme days are defined as HPD 24-h totals that exceed the USHCN top 1% wet-day threshold at each station. Shown are (a)–(c) three inland and (d)–(f) three coastal stations.

are attributed to extratropical storms (66%), and 235 (15%) are placed in the other category. For comparison, Kunkel et al. (2012) attributed 36% of annual extreme Northeast precipitation to tropical cyclones and 63% to extratropical storms (47% frontal processes, 16% extratropical cyclone centers).

The seasonal cycles of PD, PI, PT, XD, XI, and XT for each dynamical category are shown in Figs. 10 (inland stations) and 11 (coastal stations). The dashed lines indicate the combined hurricane, storm, and other category precipitation cycles. Seasonal cycles of PD are similar for coastal and inland stations, with the greatest number of storm days in winter and the least number in summer, more other category days in the warm months, and a peak in tropical cyclones in September. However, at inland stations, there are consistently more storm and other category days than at coastal stations, leading to the higher number of overall precipitation days. The XD at inland stations is greatest in summer and early fall and peaks in September because of peaks in all three dynamical categories. For coastal stations, extreme days can occur frequently throughout the year, mostly as a result of storms. For both coastal and inland stations, PI is highest for tropical cyclones, followed by storm and then other category precipitation. However, coastal and inland differences in the seasonal cycles of storm and other category PI contribute to the characteristic dual peaks of coastal PI and single peak of inland PI. Specifically, coastal storm PI decreases in June–August (JJA), while inland other category PI increases dramatically at the same time, causing a lull in overall coastal PI and a peak in overall inland PI in JJA. The XI

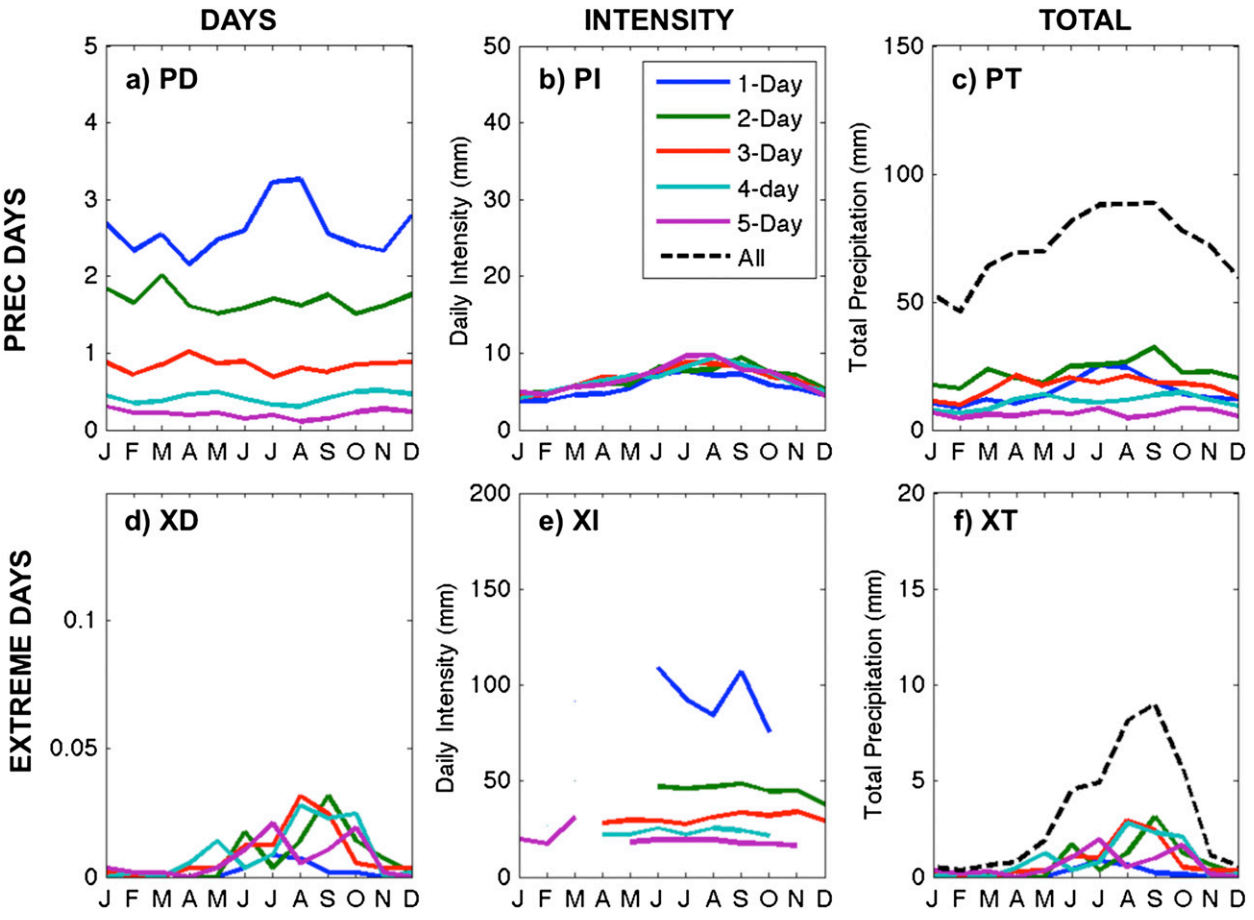

FIG. 8. Inland station annual cycle of USHCN multiday precipitation events and extreme precipitation events for event durations of 1–5 days. Shown is multiday (a) percent of PD, (b) PI, (c) PT, (d) percent of XD, (e) XI, and (f) XT. Extreme multiday events are defined as the top 1% of total event precipitation. The dashed black line in (c) and (f) shows the sum of the 1–5-day event precipitation. The noisiness of coastal XD and XT is due to small sample sizes, and the curves for different event durations cannot be considered to be statistically different.

is very similar in both magnitude and seasonality, effectively making the seasonal cycles for XT identical to the seasonal cycle of XD.

From Figs. 10 and 11, the ratios of extreme precipitation to overall precipitation can be evaluated for the dynamical categories and are similar for both coastal and inland stations (Table 4, showing annual and seasonal averages). For the hurricane category in September, tropical cyclones account for 24% of precipitation days, over 30% of total precipitation, and ~55% of extreme days and extreme precipitation. Storms account for 75%–80% of precipitation days and 80%–85% of total precipitation from December to May, as well as 45%–65% of precipitation days and 45%–75% of total precipitation from June to November. Storms account for 93%–100% of November–May extreme days and extreme precipitation and 35%–75% of June–October extreme days and extreme precipitation. Other category days account for 20%–25% of precipitation days and 15%–20% of total precipitation, except during July–August, when other category days account for over 40% of precipitation days and 35% of total precipitation. Other category days account for up to 20% of extreme days and extreme precipitation, with the exception of May, when coastal other category days account for almost 50% of extreme days and extreme precipitation. Tropical storms are slightly more efficient at producing extreme precipitation (3.4%), compared to extratropical storms (1.2%) and other category (0.4%).

f. Storm tracks and daily precipitation

Storm-related extremes make up the largest category of extreme precipitation events. In this section, storm tracks are analyzed to determine if there is a preferred track that leads to extreme precipitation. Figure 12 shows the storm-track density on storm overall precipitation

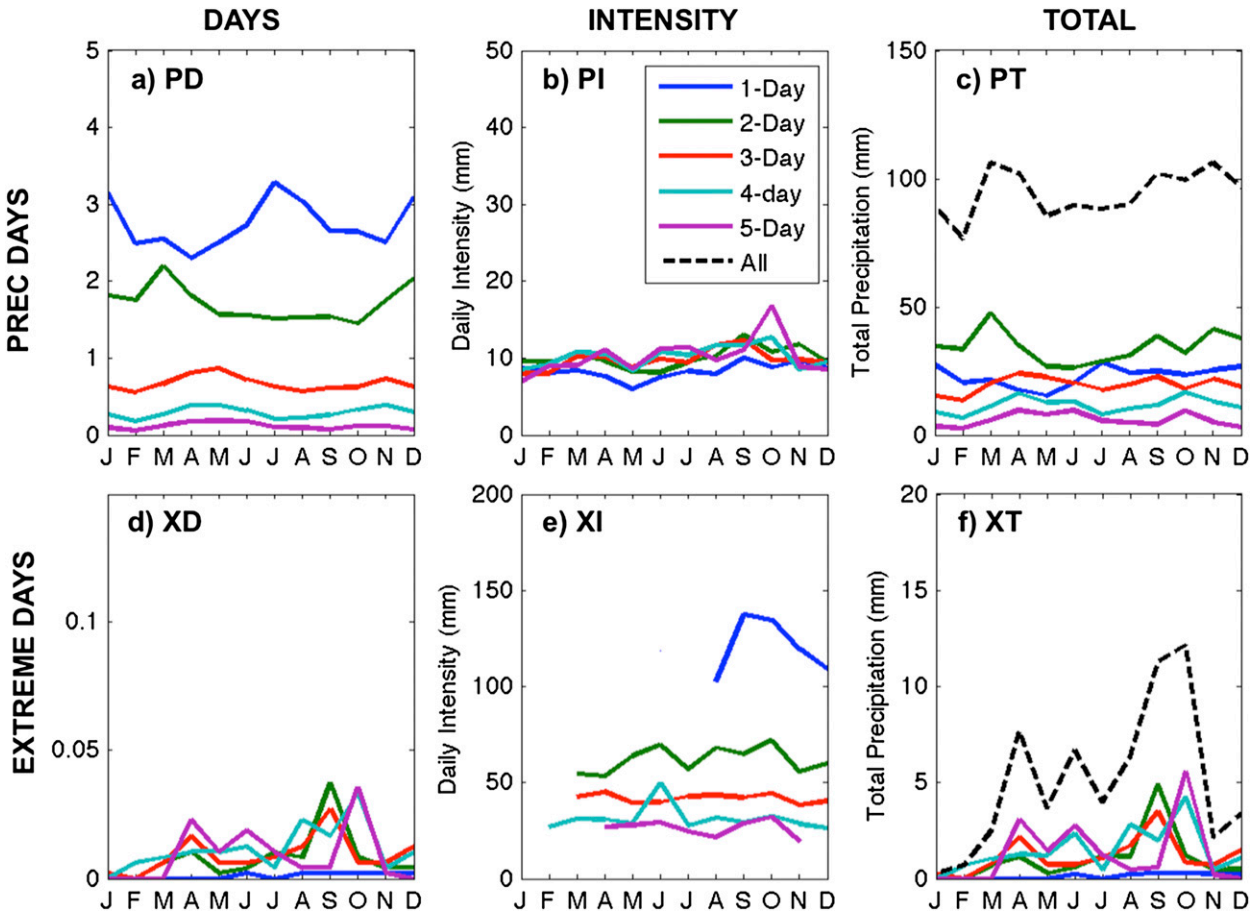

FIG. 9. As in Fig. 8, but for coastal stations. The noisiness of coastal XD and XT is partially because of the relatively small sample size.

days and storm extreme precipitation days. Track density is simply the raw count of R2 track locations that pass through each EASE grid box in the study area for each 6-h period over the 30 yr. The storm-track density is then regridded from the native EASE grid to a uniform 2.5° grid.

The storm tracks that generate overall precipitation at Northeast stations are similar between inland and coastal stations (Figs. 12a,b). In each season, there are two broad regions of strongest track density: one over the Great Lakes region, and another over the eastern seaboard, Maine, and eastern Canada. Track density is highest in DJF and March–May (MAM). In JJA and September–November (SON), the two areas of track density are weaker and shifted northward over eastern Canada.

There is less similarity between inland and coastal station storm tracks on storm-related extreme days (Figs. 12c,d). For coastal stations, there is a favored storm track from offshore New Jersey through Long Island into southern Connecticut. This favored track occurs in all seasons, although the track density is strongest in MAM and SON. The presence of the coastal track off New Jersey in JJA is somewhat surprising, since this track is usually associated with nor'easters (Kocin and Uccellini 2004), which tend to occur in fall and winter. From Figs. 11a and 11b (blue storm lines), this corresponds to a time of fewer storms but moderate-to-high precipitation intensity. Hence, when summer storms do occur along this nor'easter path (rarely), they tend to generate extreme precipitation for coastal stations.

For inland stations on storm-related extreme days, both the location and density of tracks change seasonally. Track density in DJF is similar to that for coastal stations, but with an additional slight clustering of tracks over Lake Huron. In MAM and SON, there is a strong clustering of tracks from Long Island through central New England, which is similar to the coastal track density but shifted west. Pfahl and Wernli (2012) also have noted a seasonal shifting of non-extreme tracks to the north and east during JJA, and

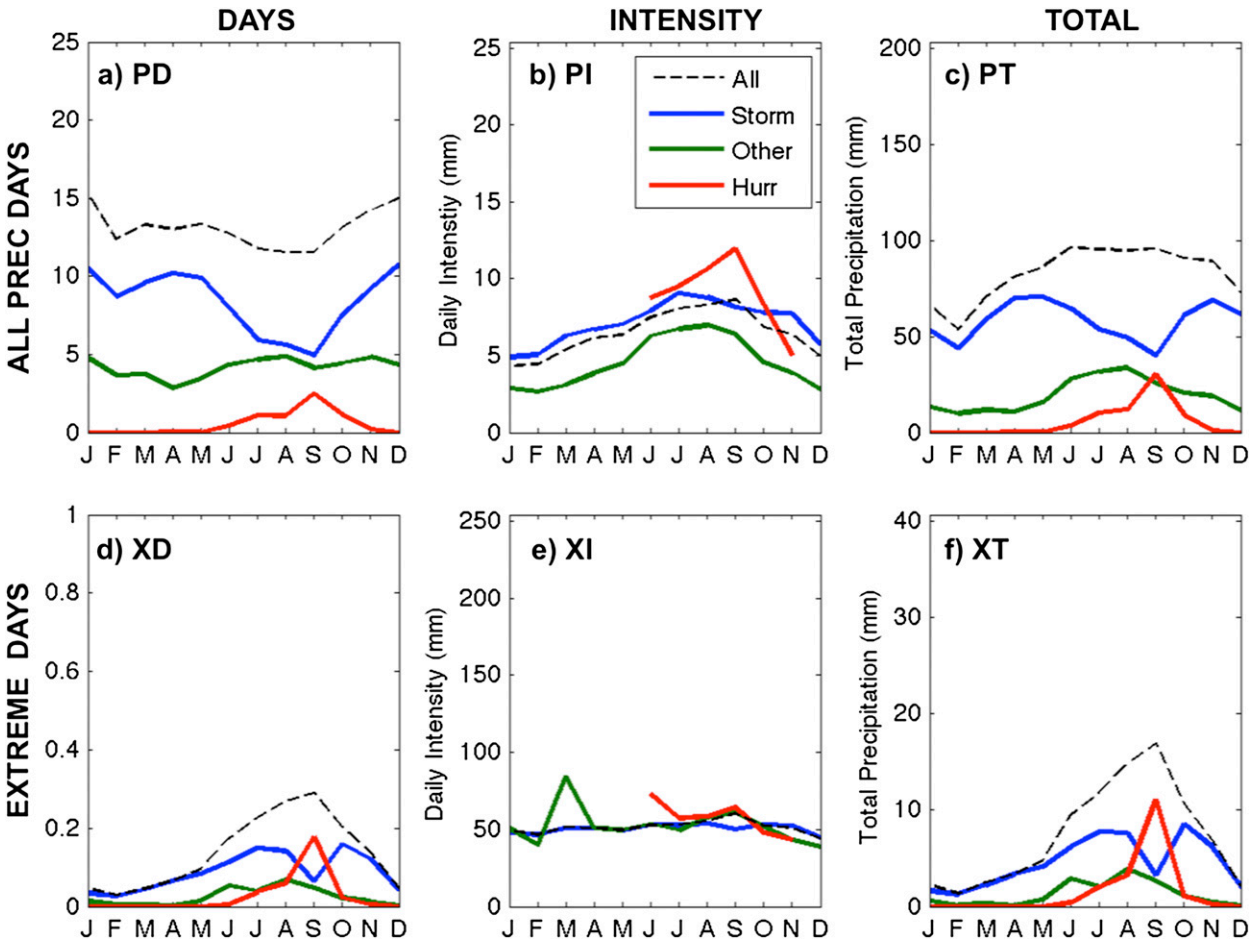

FIG. 10. Annual cycle of precipitation characteristics for inland stations, separated into dynamical categories [hurricane (red line), storm (blue line), and other (green line)]. Shown are (a) PD, (b) PI, (c) PT, (d) XD, (e) XI, and (f) XT. The dashed black lines show the sums of PD, XD, PT, and XT, respectively, and the means of PI and XI, respectively.

extreme tracks to the north and west during JJA. Interestingly, the majority of tracks occur in JJA, with a widespread area of high track density covering western and northern New England and parts of Canada, indicating many storm tracks but no single preferred storm track. This stands in contrast to coastal stations, which show few storm tracks in JJA except for the near-offshore track. From Figs. 10a and 10b (blue storm lines), the number of storms that affect inland stations decreases in the summer but storm-related precipitation intensity is at its peak, suggesting that, when storms pass anywhere through the central Northeast in the summer, the precipitation generated at inland stations can be extreme.

g. Spatial cohesiveness of extreme daily precipitation

An important measure of extreme precipitation is how widespread, or spatially cohesive, extreme precipitation is. For this study, two measures of spatial cohesiveness are considered. The first is a simple count of the number of stations reporting extreme precipitation on the same day from 1979 to 2008 (Fig. 13). Overall, 60% of extreme days occur at single stations, 90% occur at no more than 3 stations concurrently, and 97% occur at no more than 5 stations concurrently. For the hurricane category, 45% of extreme days are single-station extremes, 32% are 2- or 3-station extremes, and another 23% range from 4 to 11 stations. For the storm category, 60% of extreme days are single-station extremes, while 30% are 2- or 3-station extremes. For the other category, 77% are single-station extremes, while 15% are 2- or 3-station extremes. Not surprisingly, tropical cyclones create the most widespread extremes and the other category the least. The vast majority of other category extreme events occur at a single station, reflecting that at least some of the extreme precipitation in this category may represent mesoscale processes. This measure of spatial cohesiveness has the advantage of

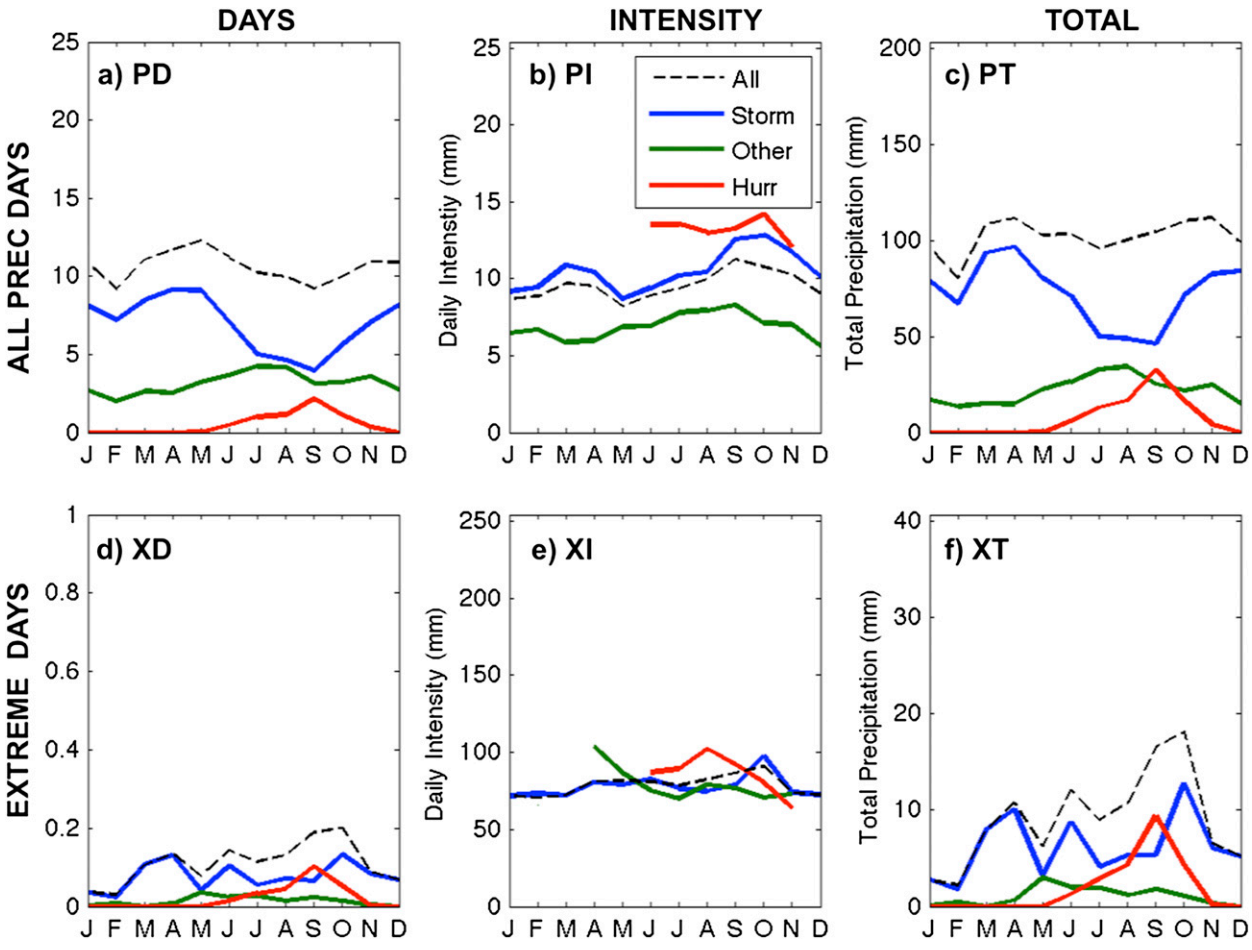

FIG. 11. As in Fig. 10, but for coastal stations.

being simple to explain, but it does not address whether stations experiencing extremes on the same day are, in fact, nearby each other, nor does it include counts from stations just outside the boundary of the Northeast domain.

The second measure of spatial cohesiveness addresses this by calculating the percent of times (hit rate) that an extreme occurs at other stations within a certain radial distance of a target station when an extreme occurs at the target station (Fig. 14). For each station j with k extreme dates and n surrounding stations, $B_1, B_2, \ldots, B_n$, the hit rate HR_j is

$$\mathrm{HR}_j = \frac{\sum_n \text{No. extremes at } B_n}{kn}(100\%). \qquad (1)$$

Radial distances of 100–500 km in 25-km increments are used, and the results are separated by dynamical category and season (radial distances less than 100 km are not included because of poor sampling). Overall, the hit rate is generally low for precipitation extremes: less than 30% at stations within 100 km, and near 10% within 500 km. Within the storm category, coastal extremes are more cohesive in SON and DJF than in MAM and JJA (30% vs 20% at 100 km); but inland extremes are more cohesive in SON only. For the other category, a seasonal breakout shows high spatial cohesiveness in MAM but very low spatial cohesiveness (5% within 100 km) in JJA, consistent with convection or other mesoscale processes. The high hit rate in MAM may be caused by sampling error, since very few other category events occur during MAM. Hurricane category extremes appear to be slightly more spatially cohesive than storm category extremes (30%–40% at 100 km). For the hurricane category, inland cohesiveness is generally stronger than coastal cohesiveness, while for the storm category, the opposite is true. It should be noted that this measure of spatial cohesiveness is somewhat sensitive to clustering of stations, since inland stations are somewhat farther apart than coastal stations, and sample size is reduced as radial distance decreases. In addition, inland stations are located in regions of varying topography and

TABLE 4. Percent of precipitation days and total precipitation for dynamical categories of tropical storms, extratropical storms, and other, based on coastal monthly climatology shown in Figs. 10 and 11 (e.g., for SON, tropical cyclones account for 12.7% of precipitation days but only 0.5% of SON precipitation days are extreme because of tropical cyclones, while 27.4% of all extreme precipitation days are caused by tropical cyclones, but only 3.3% of all tropical cyclone days involve extreme precipitation). Inland results are similar. All values are percentages.

	Precipitation due to category (%)		Precipitation that is extreme because of category (%)		Extreme precipitation due to category (%)		Category precipitation that is extreme (%)	
Category	PD	PT	PD	PT	PD	PT	PD	PT
Tropical cyclone								
JJA	8.4	12.0	0.3	2.9	24.7	27.7	3.5	23.1
SON	12.7	16.8	0.5	4.3	27.4	27.5	3.3	19.1
Extratropical storm								
Annual	64.8	71.2	0.7	5.8	74.7	74.3	1.2	8.6
DJF	76.0	83.5	0.4	3.5	93.3	93.8	0.6	4.1
MAM	76.2	83.6	0.8	6.5	83.1	81.9	1.0	7.7
JJA	52.9	56.6	0.7	6.0	57.9	56.1	1.4	10.5
SON	54.4	61.1	0.9	7.4	64.6	65.3	1.7	12.3
Other								
Annual	29.9	21.6	0.1	1.0	12.2	11.9	0.4	4.2
DJF	24.0	16.5	0.0	0.2	6.7	6.2	0.1	1.0
MAM	23.8	16.4	0.1	1.2	16.9	18.1	0.5	5.9
JJA	38.7	31.4	0.2	1.7	17.4	16.2	0.6	5.6
SON	32.9	22.1	0.1	1.0	8.0	7.2	0.4	4.4

geographic conditions, whereas coastal stations all lie within the relatively homogenous coastal plain. These problems make it difficult to accurately assess the differences in coastal and inland spatial cohesiveness without additional analysis. However, although scale and cohesiveness are not identical concepts, and, more importantly, station-based extremes are not necessarily related to measures of extreme precipitation on larger scales, our results are consistent with Konrad (2001) in that precipitation extremes associated with storms and hurricanes are often small-scale events in the Northeast.

4. Summary and discussion

This study examines the climatology of U.S. Northeast daily precipitation and extreme (top 1% of wet days) daily precipitation in terms of seasonal and spatial distribution, time scale, and relation to large-scale factors, based on daily station data from 1979 to 2008. Regional precipitation characteristics are identified, and regional monthly climatologies of frequency, intensity, and total precipitation are developed for both daily and multiday precipitation events. Daily precipitation events are then categorized into dynamical groupings based on proximity to tropical cyclones or extratropical storm centers, and the climatologies of overall and extreme daily precipitation are developed for each dynamical category. Seasonal shifts in storm tracks are identified for extratropical storm–related precipitation and extreme precipitation days. Finally, the spatial scale of extreme precipitation is explored for each category. Each of these aspects of Northeast precipitation is important to understand on its own, but together the results help to create a larger-picture view of the climatology of precipitation in the region and give us better insight into the specific results.

There are several key results from this study:

- For spatial distribution, there are two Northeast subregions with distinct precipitation characteristics. The inland region includes more days of precipitation and weaker intensity, with peak days in winter and peak intensity in summer. The coastal region includes fewer days of precipitation and stronger intensity, with peak days in spring and late fall and peak intensity in early spring and fall.
- For seasonality, the majority of extreme precipitation days in the Northeast occur from April to October; however, extreme days can occur in any month, and the intensity on extreme days is equally high regardless of season.
- For time scale, 50% of overall precipitation occurs as single-day events. However, most extreme precipitation in the Northeast occurs during multiday precipitation events of 2–5 days, in which only a single day within the event is actually extreme, and only 1–3 h account for approximately 50% of the daily accumulation.
- For large-scale factors, extratropical storm–related precipitation is the strongest driver of the seasonal cycle of Northeast overall precipitation and extreme

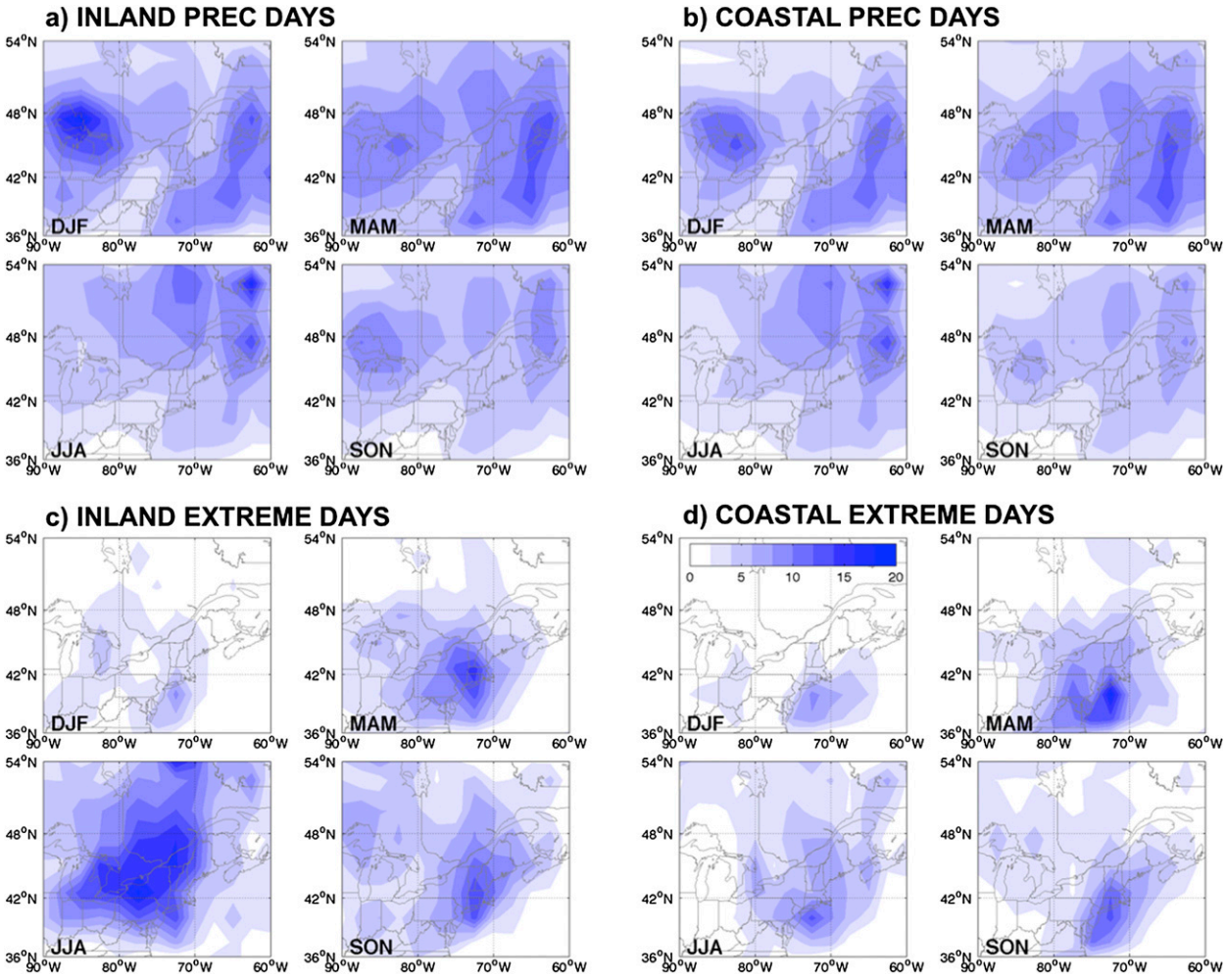

FIG. 12. Storm-track density on storm-related precipitation days. The total number of R2 tracks that pass through each grid location by season for (a) inland overall precipitation days, (b) coastal overall precipitation days, (c) inland extreme precipitation days, and (d) coastal extreme precipitation days. Duplicate dates (e.g., extremes at multiple stations on same date) are only counted once.

precipitation frequency, intensity, and totals. Extratropical storms account for 80%–85% of total precipitation from December to May and 93%–100% of extreme precipitation from November to May. The characteristic dual peak in coastal overall precipitation intensity and total is related to the lull in storm-related intensity in May.

- As another key aspect of spatial distribution, Northeast extreme precipitation events have low spatial cohesion (here, referring to how widespread a precipitation event is), with most extreme precipitation occurring at single stations. Tropical cyclone–related extremes show the most spatial cohesiveness, storm-related extremes show less spatial cohesiveness, and other category extremes (likely convective events) show even less spatial cohesiveness. Coastal extremes appear to be more spatially cohesive than inland extremes for storms but less spatially cohesive than inland extremes for tropical cyclones.

These findings raise some interesting questions, both with respect to the specific results and to the underlying dynamics that cause precipitation and extreme precipitation in the Northeast.

One basic question raised by these results is what causes the differences in coastal and inland precipitation characteristics. The proximity of coastal stations to open water can enhance the availability of water vapor content and account for the higher precipitation intensity at coastal stations throughout the year (Marks and Austin 1979). The warm-month increase in intensity is likely caused by the temperature dependence on water vapor content, which appears fully realized at inland stations but is moderated at coastal stations by cooler water

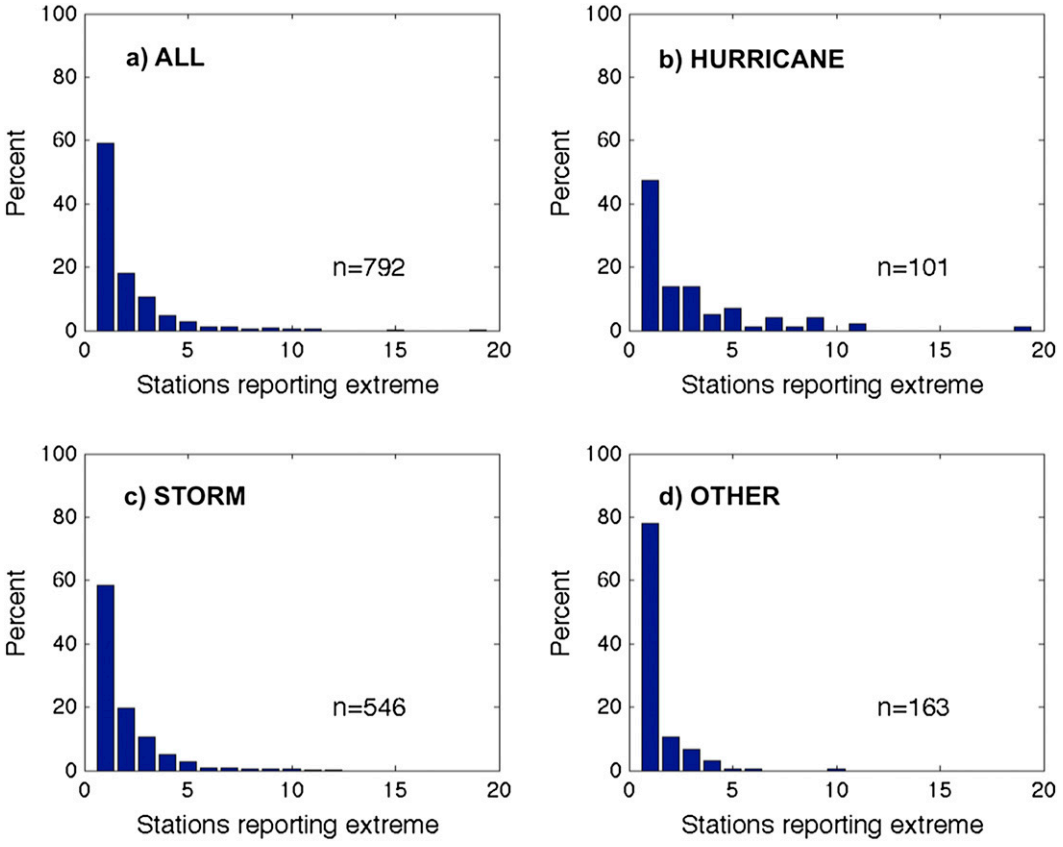

FIG. 13. Percent of extreme precipitation days experienced at multiple stations for (a) all extremes days, (b) hurricane-related precipitation days, (c) storm-related precipitation days, and (d) other category–related precipitation days. Also shown is the number of unique extreme precipitation dates for the category.

temperatures and sea breezes (Trenberth et al. 2003). This may partly account for the spring lull in coastal intensity. The high number of light precipitation days at inland stations is likely influenced by winter lake-effect precipitation, orographic forcing, localized convection, blocking episodes, and backdoor cold fronts, which are active in late spring and early summer and can contribute to consecutive days of drizzle (Bosart et al. 1973). As we have shown, extratropical storms strongly influence the seasonal cycles at inland and coastal stations. It is possible that the lull in coastal precipitation intensity in May, despite the high number of days of storm-related precipitation, is related to the shifting of the jet stream to a more northerly position (a reduction in nor'easter-type storms) in conjunction with a delay in warming caused by proximity to cold ocean temperatures. In addition, the increase in precipitation intensity at inland stations during JJA may be related to storm-related frontal processes triggering or interacting with background conditions to create stronger convective events.

Another question is why Northeast precipitation spatial cohesiveness is not higher, considering the frequency of extratropical and tropical storms affecting the region. Coastal cohesiveness may be related to nor'easter-type storm systems that travel along the coast affecting a broad area (Hawcroft et al. 2012), while inland cohesiveness may be more influenced by embedded convective systems (Murray and Colle 2011). Regardless of larger-scale context, it appears likely that mesoscale processes play an important role in extreme station precipitation, whether standalone (convection) or embedded in larger systems, such as synoptic storms and tropical storms (banding).

A final question is why extreme precipitation intensity is uniformly strong, regardless of season. This suggests that the ingredients for extreme precipitation (presumably including water vapor availability and strength of vertical ascent) can be present in any season, regardless of specific circulation patterns, mean temperatures, and dynamical forcing mechanisms. It is not clear whether the cool-season circulation patterns and dynamical forcing

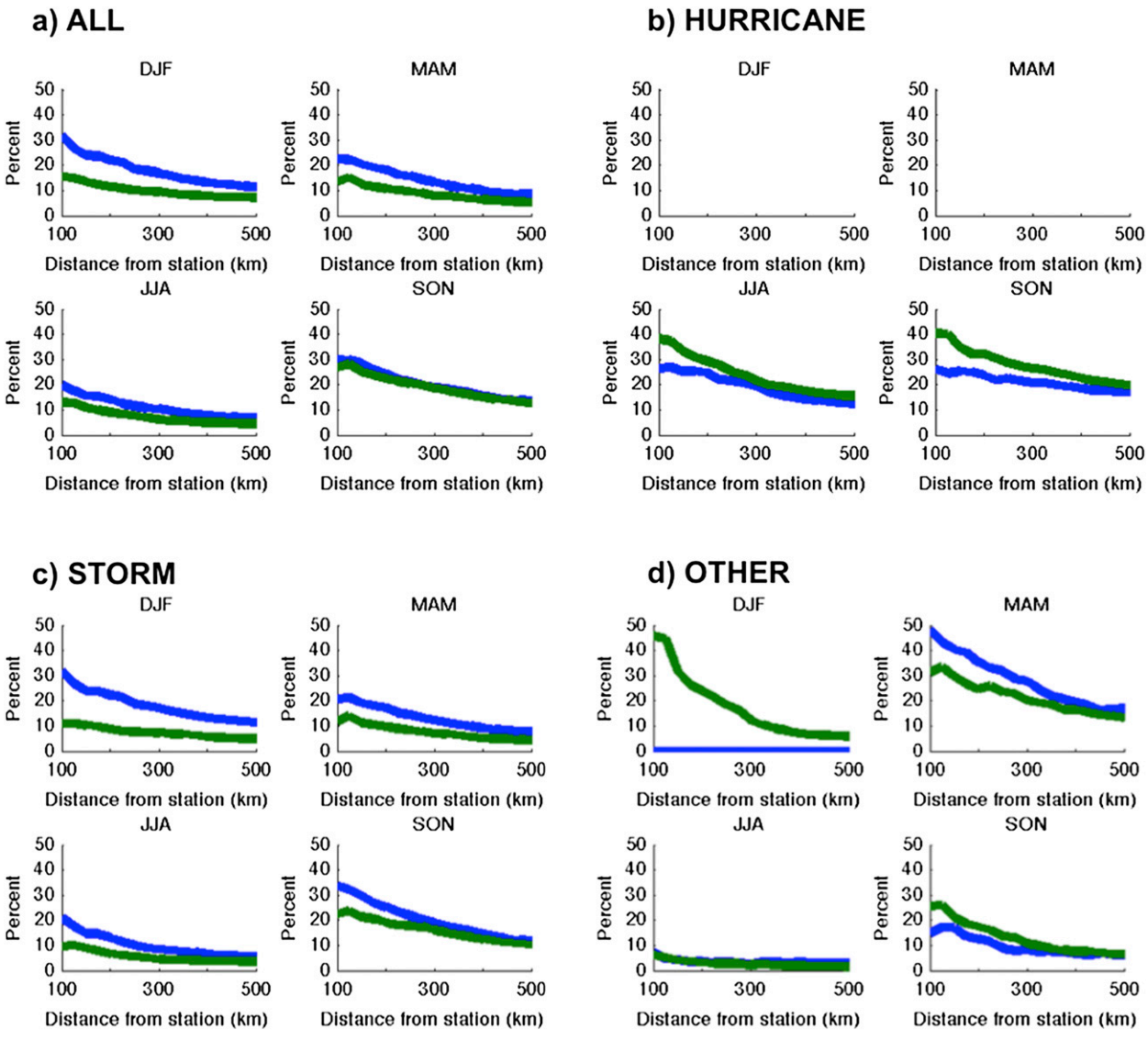

FIG. 14. Hit rate of extremes experienced at nearby stations, by category and season. For the four seasons and at varying distances from target stations, shown are (a) all extreme days, (b) hurricane-related precipitation extreme days, (c) storm-related precipitation extreme days, and (d) other category–related precipitation extreme days.

mechanisms that lead to extreme precipitation are less frequent or less potent than those that cause warm-season extremes.

These questions highlight the importance of gaining a better understanding of the underlying dynamics of extreme precipitation events in the Northeast. We are currently pursuing a range of approaches to address these issues, including formal pattern-based typing of meteorological fields on extreme days, investigation of dynamical fields during other category–related precipitation, detailed analysis of the role of extratropical storm fronts in creating extreme precipitation, consideration of multistorm interactions (especially tropical and extratropical storm interaction), and investigation into the role of moisture and ascent for specific extreme events, as well as for the broader collection of extreme events.

Acknowledgments. This work was supported by NSF Grant 0811099 and NASA Grant NNX13AN36G.

REFERENCES

Anagnostopoulou, C., and K. Tolika, 2012: Extreme precipitation in Europe: Statistical threshold selection based on climatological criteria. *Theor. Appl. Climatol.*, **107**, 479–489, doi:10.1007/s00704-011-0487-8.

Armstrong, R. L., and M. J. Brodzik, 1995: An Earth-gridded SSM/I data set for cryospheric studies and global change monitoring. *Adv. Space Res.*, **16**, 155–163, doi:10.1016/0273-1177(95)00397-W.

Barlow, M., 2011: Influence of hurricane-related activity on North American extreme precipitation. *Geophys. Res. Lett.*, **38**, L04705, doi:10.1029/2010GL046258.

Beguería, S., M. Angulo-Martínez, S. Vicente-Serrano, J. I. López-Moreno, and A. El-Kenawy, 2011: Assessing trends in extreme precipitation events intensity and magnitude using non-stationary peaks-over-threshold analysis: A case study in northeast Spain from 1930 to 2006. *Int. J. Climatol.*, **31**, 2102–2114, doi:10.1002/joc.2218.

Bosart, L. F., V. Pagnotti, and B. Lettau, 1973: Climatological aspects of eastern United States back-door cold frontal passages. *Mon. Wea. Rev.*, **101**, 627–635, doi:10.1175/1520-0493(1973)101<0627:CAOEUS>2.3.CO;2.

Catto, J. L., and S. Pfahl, 2013: The importance of fronts for extreme precipitation. *J. Geophys. Res. Atmos.*, **118**, 10 791–10 801, doi:10.1002/jgrd.50852.

——, C. Jakob, G. Berry, and N. Nicholls, 2012: Relating global precipitation to atmospheric fronts. *Geophys. Res. Lett.*, **39**, L10805, doi:10.1029/2012GL051736.

DeGaetano, A. T., 2009: Time-dependent changes in extreme-precipitation return-period amounts in the continental United States. *J. Appl. Meteor. Climatol.*, **48**, 2086–2099, doi:10.1175/2009JAMC2179.1.

Douglas, E. M., and C. A. Fairbank, 2011: Is precipitation in northern New England becoming more extreme? Statistical analysis of extreme rainfall in Massachusetts, New Hampshire, and Maine and updated estimates of the 100-year storm. *J. Hydrol. Eng.*, **16**, 203–217, doi:10.1061/(ASCE)HE.1943-5584.0000303.

Easterling, D. R., T. R. Karl, J. H. Lawrimore, and S. A. Del Greco, 1999: United States Historical Climatology Network daily temperature, precipitation, and snow data for 1871–1997. ORNL/CDIAC-118, NDP-070. Carbon Dioxide Information Analysis Center, accessed 25 June 2012. [Available online at http://gcmd.nasa.gov/records/GCMD_CDIAC_NDP070.html.]

Federal Emergency Management Agency, 2006: Mass. disaster aid surpasses $70 million for May floods. [Available online at http://www.fema.gov/news-release/2006/09/22/mass-disaster-aid-surpasses-70-million-may-floods.]

Griffiths, M. L., and R. S. Bradley, 2007: Variations of twentieth-century temperature and precipitation extreme indicators in the Northeast United States. *J. Climate*, **20**, 5401–5417, doi:10.1175/2007JCLI1594.1.

Hawcroft, M. K., L. C. Shaffrey, K. I. Hodges, and H. F. Dacre, 2012: How much Northern Hemisphere precipitation is associated with extratropical cyclones? *Geophys. Res. Lett.*, **39**, L24809, doi:10.1029/2012GL053866.

Hitchens, N. M., R. J. Trapp, M. E. Baldwin, and A. Gluhovsky, 2010: Characterizing subdiurnal extreme precipitation in the midwestern United States. *J. Hydrometeor.*, **11**, 211–218, doi:10.1175/2009JHM1129.1.

Kanamitsu, M., W. Ebisuzaki, J. Woollen, S. K. Yang, J. J. Hnilo, M. Fiorino, and G. L. Potter, 2002: NCEP–DOE AMIP-II Reanalysis (R-2). *Bull. Amer. Meteor. Soc.*, **83**, 1631–1643, doi:10.1175/BAMS-83-11-1631.

Kenyon, J., and G. C. Hegerl, 2010: Influence of modes of climate variability on global precipitation extremes. *J. Climate*, **23**, 6248–6262, doi:10.1175/2010JCLI3617.1.

Kocin, P. J., and L. W. Uccellini, 2004: *Northeast Snowstorms. Meteor. Monogr.*, No. 54, Amer. Meteor. Soc., 818 pp.

Konrad, C. E., II, 2001: The most extreme precipitation events over the eastern United States from 1950 to 1996: Considerations of scale. *J. Hydrometeor.*, **2**, 309–325, doi:10.1175/1525-7541(2001)002<0309:TMEPEO>2.0.CO;2.

Kunkel, K. E., K. Andsager, and D. R. Easterling, 1999: Long-term trends in extreme precipitation events over the conterminous United States and Canada. *J. Climate*, **12**, 2515–2527, doi:10.1175/1520-0442(1999)012<2515:LTTIEP>2.0.CO;2.

——, D. R. Easterling, D. A. R. Kristovich, B. Gleason, L. Stoecker, and R. Smith, 2012: Meteorological causes of the secular variations in observed extreme precipitation events for the conterminous United States. *J. Hydrometeor.*, **13**, 1131–1141, doi:10.1175/JHM-D-11-0108.1.

——, and Coauthors, 2013a: Monitoring and understanding trends in extreme storms: State of knowledge. *Bull. Amer. Meteor. Soc.*, **94**, 499–514, doi:10.1175/BAMS-D-11-00262.1.

——, and Coauthors, 2013b: Regional climate trends and scenarios for the U.S. National Climate Assessment. Part 1. Climate of the Northeast U.S., NOAA Tech. Rep. NESDIS 142-1, 80 pp. [Available online at http://www.nesdis.noaa.gov/technical_reports/NOAA_NESDIS_Tech_Report_142-1-Climate_of_the_Northeast_U.S.pdf.]

Landsea, C. W., and J. L. Franklin, 2013: Atlantic hurricane database uncertainty and presentation of a new database format. *Mon. Wea. Rev.*, **141**, 3576–3592, doi:10.1175/MWR-D-12-00254.1.

Lenderink, G., H. Y. Mok, T. C. Lee, and G. J. Van Oldenborgh, 2011: Scaling and trends of hourly precipitation extremes in two different climate zones—Hong Kong and the Netherlands. *Hydrol. Earth Syst. Sci.*, **15**, 3033–3041, doi:10.5194/hess-15-3033-2011.

Lott, N., and T. Ross, 2006: Tracking and evaluating U. S. billion dollar weather disasters, 1980–2005. *AMS Forum: Environmental Risk and Impacts on Society: Successes and Challenges*, Atlanta, GA, Amer. Meteor. Soc., 1.2. [Available online at https://ams.confex.com/ams/Annual2006/techprogram/paper_100686.htm.]

Marks, F. D., and P. M. Austin, 1979: Effects of the New England coastal front on the distribution of precipitation. *Mon. Wea. Rev.*, **107**, 53–67, doi:10.1175/1520-0493(1979)107<0053:EOTNEC>2.0.CO;2.

Melillo, J. M., T. C. Richmond, and G. W. Yohe, 2014: *Climate Change Impacts in the United States: The Third National Climate Assessment.* U.S. Global Change Research Program, 841 pp., doi:10.7930/J0Z31WJ2.

Michelangeli, P., R. Vautard, and B. Legras, 1995: Weather regimes: Recurrence and quasi stationarity. *J. Atmos. Sci.*, **52**, 1237–1256, doi:10.1175/1520-0469(1995)052<1237:WRRAQS>2.0.CO;2.

Murray, J. C., and B. A. Colle, 2011: The spatial and temporal variability of convective storms over the Northeast United States during the warm season. *Mon. Wea. Rev.*, **139**, 992–1012, doi:10.1175/2010MWR3316.1.

NOAA, 2014: HURDAT Re-Analysis Project. Hurricane Research Division, Atlantic Oceanographic and Meteorological Laboratory, accessed 13 February 2014. [Available online at http://www.aoml.noaa.gov/hrd/hurdat/Data_Storm.html.]

——, 2015: Billion-dollar weather and climate disasters: Table of events. [Available online at http://www.ncdc.noaa.gov/billions/events.]

Peterson, T. C., and Coauthors, 2013: Monitoring and understanding changes in heat waves, cold waves, floods, and droughts in the United States: State of knowledge. *Bull. Amer. Meteor. Soc.*, **94**, 821–834, doi:10.1175/BAMS-D-12-00066.1.

Pfahl, S., and H. Wernli, 2012: Quantifying the relevance of cyclones for precipitation extremes. *J. Climate*, **25**, 6770–6780, doi:10.1175/JCLI-D-11-00705.1.

Pryor, S. C., J. A. Howe, and K. E. Kunkel, 2009: How spatially coherent and statistically robust are temporal changes in extreme precipitation in the contiguous USA? *Int. J. Climatol.*, **29**, 31–45, doi:10.1002/joc.1696.

Ralph, F. M., E. Sukovich, D. Reynolds, M. Dettinger, S. Weagle, W. Clark, and P. J. Neiman, 2010: Assessment of extreme quantitative precipitation forecasts and development of regional extreme event thresholds using data from HMT-2006 and COOP observers. *J. Hydrometeor.*, **11**, 1286–1304, doi:10.1175/2010JHM1232.1.

Serreze, M. C., 1995: Climatological aspects of cyclone development and decay in the Arctic. *Atmos.–Ocean*, **33**, 1–23, doi:10.1080/07055900.1995.9649522.

——, F. Carse, R. G. Barry, and J. C. Rogers, 1997: Icelandic low cyclone activity: Climatological features, linkages with the NAO, and relationships with recent changes in the Northern Hemisphere circulation. *J. Climate*, **10**, 453–464, doi:10.1175/1520-0442(1997)010<0453:ILCACF>2.0.CO;2.

Trenberth, K. E., A. Dai, R. M. Rasmussen, and D. B. Parsons, 2003: The changing character of precipitation. *Bull. Amer. Meteor. Soc.*, **84**, 1205–1217, doi:10.1175/BAMS-84-9-1205.

Tryhorn, L., and A. DeGaetano, 2011: A comparison of techniques for downscaling extreme precipitation over the Northeastern United States. *Int. J. Climatol.*, **31**, 1975–1989, doi:10.1002/joc.2208.

Yiou, P., K. Goubanova, Z. X. Li, and M. Nogaj, 2008: Weather regime dependence of extreme value statistics for summer temperature and precipitation. *Nonlinear Processes Geophys.*, **15**, 365–378, doi:10.5194/npg-15-365-2008.